

**Fate of Emerging Nanoparticle Contaminants during Aquifer Recharge with Treated Wastewater (Project # 2012AZ476B)**

Reyes Sierra-Alvarez Jim A Field  
Department of Chemical and Environmental Engineering  
The University of Arizona (E-mail: email:rsierra@email.arizona.edu)

**A. Problem and Research Objectives**

**A.i) Background**

*Nanoparticles and their applications.* Nanoparticles (NPs) can be defined as particles with at least one dimension less than 100 nm. Nanoparticles offer a diversity of new technological possibilities for a rapidly growing nanotechnology sector [1], and they can now be found in consumer products (e.g. sun screen, cosmetics, bactericidal agents, medicines, printing ink, computer chips) [2], and in industrial effluents [5-6]. Titanium dioxide (TiO<sub>2</sub>) is widely used for their photolytic properties [3]. TiO<sub>2</sub> is a photocatalyst that has been used in solar cells, paints, and coatings, and it is widely used in sunscreens and cosmetics [4].

*Public health and environmental impacts:* Concern among scientists and regulatory agencies about the potential negative impacts of NPs on human health and the environment is growing as a result of increasing emissions of engineered NPs resulting from their greater application in industrial processes and consumer products. Studies conducted over the past 10 years have provided compelling evidence that a variety of engineered NPs, including metal oxides, fullerenes and carbon nanotubes, can cause toxic effects to mammalian cells [7-9] and other living organisms ranging from bacteria and other aquatic organisms to terrestrial plants [4,10-12]. NPs have been shown to cause disruption of cell membranes, oxidation of proteins, genotoxicity, formation of reactive oxygen species, and release of toxic species [4,13,16]. There is also evidence that NPs can be taken up by cells [13-14] and become systemically distributed throughout the body [13,15].

*Environmentall fate of NPs:* The concentrations of engineered NPs in natural waters are as yet unknown. Nonetheless, simple box models have predicted concentrations of the most common NPs (Ag and oxides of Ti, Ce, and Zn) in natural waters in the range 1 to 10 µg/L, and total NP concentrations approaching as much as 100 µg/L [36]. In spite of the increasing need to evaluate the effects that NPs may have on the environment, few studies have investigate the transport and fate of nanomaterials in aquatic and terrestrial environments, and little is known regarding interactions of NPs with environmental matrices. NP transport experiments have focused primarily on enhancing delivery of zero-valent iron (ZVI) to soil and groundwater for remediation purposes [32, 37]. Recent studies have also considered the transport of a few other engineered NPs in porous media [38-39].

*Fate of NPs in wastewater treatment plants:* A significant fraction of engineered NPs can be expected to reach municipal and industrial wastewater treatment plants (WWTPs) since large fractions of these nanomaterials are released to sewer systems [17]. This was recently demonstrated based on a model that considered the environmental fate of various engineered NPs once released from consumer products or industrial processes [18]. Evidence of the occurrence of NPs in municipal WWTPs includes the detection of TiO<sub>2</sub> NPs in the treated effluent from several treatment plants in the USA [19] at concentrations ranging from < 5 to 15 µg/L, and the detection of silver sulfide NPs in sewage sludge from a full-scale municipal WWTP [20]. The release of nano-silver into wastewater from a facility manufacturing nano-Ag containing consumer products (socks with bactericidal silver) has also been observed [21]. The question of whether conventional WWTPs remove NPs has not been examined very thoroughly. Although information on the fate on NPs in WWTP is still very scant, preliminary results [19,22-23] suggest that effluent discharges could represent a significant input of NP into the environment. In locations such as Tucson and other cities in Arizona where aquifer recharge of treated effluents is practiced, NPs carried by the wastewater could potentially be transported to groundwater used for drinking water supply. Therefore, characterization of the fate and behavior of NPs in porous media is needed to quantify exposure scenarios.

## **A.ii) Objectives**

The objective of this research is to determine the extent to which engineered NPs in treated wastewater are attenuated by soil-aquifer treatment. In arid and semiarid environment, aquifer recharge will occur either intentionally (soil-aquifer treatment) or unintentionally (via discharge of effluent to a dry river or discharge via septic drainage fields). One of the aims is to quantify the attenuation of NPs during transport through porous sediment medium. A second aim is to understand the role of organic matter in treated wastewater on the fate of NPs in porous media.

## **B. Methodology**

### **B.i) Work plan**

The proposal included two interrelated tasks as described below:

*1. NP characterization.* Extensive characterization of the NPs is necessary to interpret fate and transport data. The chemical composition, surface chemistry, specific surface area, crystallinity, particle size and shape, size distribution, agglomeration state, surface charge/zeta potential of TiO<sub>2</sub> NPs will be evaluated as described in the Materials & Methods section.

*2. Fate and transport of TiO<sub>2</sub> NPs in porous media: Impact of reclaimed water.* The objective of this task is to assess the impact of model wastewater constituents on NP transport. Three contaminants were used to simulate varying contaminants commonly found in aqueous streams. The model organic compounds selected included a non-ionic surfactant, (Triton X-100), an anionic surfactant (ammonium polyacrylate, Dispex A40, BASF, Freeport, TX, USA), a protein (lysozyme, from Sigma-Aldrich) and an aminoacid (glycine from Sigma Aldrich).

## **B.ii) Materials and methods**

Nanomaterials. Nano-sized TiO<sub>2</sub> (21 nm, Aeroxide P25) was obtained from Evonik Industries (Essen, Germany).

Porous media. Quartz sand with an average diameter of 190 μm was obtained from Acros Organics (Geel, Belgium). The sand was sieved to remove fines and oversized material and then washed several times with acid (HCl, 5%) to eliminate metal oxides coating that could alter its surface chemistry. Subsequently the sand was rinsed with deionized water, and dried for 8 h at 105°C.

Adsorption Isotherms. Batch experiments for determining equilibrium isotherms of the TiO<sub>2</sub> NPs with the three bed materials were conducted in duplicate using a weak phosphate buffer solution (0.5 mM, pH 7, 1.0 mM ionic strength) in glass serum flasks (166 mL) at room temperature (23±2°C). The solution volume was 50 mL and the initial NP concentration ranged from 5–200 mg/L. From 0.1 to 1.0 g of bed material was added to each flask. NP-free and porous media-free controls were performed concurrently to account for any titanium (Ti) leached from the porous media and for any TiO<sub>2</sub> removal mechanisms not mediated by the media, respectively. Samples were taken of the supernatant both initially and after 3 days of stirring at 150 rpm, which a kinetic study proved to be sufficient time to reach equilibrium. Samples for titanium analysis were taken after allowing the suspensions to rest for 30 min to ensure the settling of the adsorptive media. The amount of TiO<sub>2</sub> adsorbed was determined by mass balance upon correction for any TiO<sub>2</sub> settling observed in the media-free control.

Transport studies - Experiments were performed in similar fashion to previously published methods [52] using a glass column (inner diameter= 15 mm, length= 150 mm, Omnifit Benchmark, Diba Industries, Danbury, CT, USA) packed with sand at room temperature (23±2°C). Two flow-through quartz cuvettes with 10 mm path lengths (Starna Cells, Inc., Atascadero, CA, USA) were connected to the column influent and effluent using 0.159 cm diameter PTFE tubing. A UV-Vis spectrophotometer (UV 1800, Shimadzu Corporation, Kyoto, Japan) provided absorption data, at 300 nm, monitored by an attached computer at 10 sec intervals. Flow rate control was achieved using a peristaltic pump (Micropuls3, Gilson, Inc., Middleton, WI, USA). Sand columns were dry-packed with 36.5 g of pre-washed sand under agitation from an ultrasonic bath. The column was then filled from the bottom with deionized water at a rate of 2.6 mL/min for 30 min in an ultrasonic bath to ensure wetting of the bed.

A weak phosphate buffer (0.5 mM, pH 7, 1 mM ionic strength) was prepared and any contaminants, when applicable, were added prior to final pH adjustment. Both pH and conductivity measurements were taken for each preparation. A portion of this solution was then separated to pre-rinse the column, displacing 5 bed volumes, so that the conditions on the column were identical to those in the NP suspension. Suspensions of n-TiO<sub>2</sub> (50 mg/L) were prepared in the previously prepared buffer solution by adding the appropriate amount of NPs to 50 mL centrifuge tubes filled with approximately 45 mL of the background solution. These were then sonicated (Ultrasonic Processor, Cole-Parmer, Vernon Hills, IL, USA, 65% intensity, 5 min) and recombined under constant stirring. Both pH and conductivity measurements were again performed to ensure continuity between experimental runs. The NP suspension was pumped through the column at a rate of 2.6 mL/min for 30 bed volumes. Concurrently, samples

were taken at 10 bed volume intervals and tested for size distribution and zeta potential. After 30 bed volumes, the column was rinsed for 5 bed volumes with the background solution. Samples of the column media were then taken at five locations equidistant throughout the column starting at the inlet in order to determine the amount of retained NPs associated with the column media. These experiments were performed in triplicate.

*Nanoparticle dispersion stability.* The stability of NP dispersions was evaluated by monitoring their particle size distribution (PSD) and zeta potential. Additional information will be obtained by allowing samples to settle for 30-45 min under static conditions, and analyzing samples of the supernatant for PSD, zeta potential, and the concentration of Ti. Samples of the supernatant will be collected carefully to avoid carryover of any settled material.

*Analyses.* Liquid samples (1 mL) containing TiO<sub>2</sub> were digested in a microwave digester for 30 min at 151°C (25 min ramp time, 1,600 W power) using a mixture of 71% HNO<sub>3</sub> (5 mL) and H<sub>2</sub>SO<sub>4</sub> (5 mL) for TiO<sub>2</sub> samples. Soluble Ti was measured by inductively-coupled plasma-optical emission spectrometry (Optima 2100 DV instrument, Perkin-Elmer). NP morphology will be characterized by transmission electron microscopy using a Hitachi S-4800 instrument at 15 kV voltage. The specific surface area of the NPs will be determined using a BET analyzer. The surface chemistry and crystallinity of the NPs will be characterized using X-ray photoelectron spectroscopy (Kratos 165 Ultra XPS) and XR diffractometer (Scintag XDS 2000 PTS), respectively. NP solubility will be determined by filtration through a 1-nm cutoff membrane.

The zeta potential of NPs in aqueous solution will be measured with a Zeta Sizer Nano ZS instrument (Malvern, Inc.) using the Smoluchowski equation to correlate particle electrophoretic mobility to zeta potential. Particle size distribution measurements will be determined by dynamic light scattering using the same instrument. Wastewater analysis (pH, chemical oxygen demand, BOD, suspended solids, alkalinity, etc.) will be performed according to standard methods [35].

NPs were imaged by transmission electron microscope using a Hitachi H8100 at 200 keV. Surface area measurements were obtained by nitrogen gas adsorption using a Beckman Coulter SA 3100 (Beckman Coulter, Inc., Brea, CA) and the pore distribution data was deduced using a cylindrical pore model.

## **C. Principal findings and significance**

### ***C.i) NP characterization***

Transmission electron microscopy imaging of the n-TiO<sub>2</sub> displayed crystalline and nearly spherical particles (Fig 1). The TiO<sub>2</sub> NPs (dry powder) had a reported primary particle size of 21 nm. The average particle size of n-TiO<sub>2</sub> in aqueous solution at pH 7 was significantly higher (200±2 nm) suggesting some aggregation (Fig. 2). At the same pH value, the zeta potential of n-TiO<sub>2</sub> was very low (-41.7±3.7 mV), which is indicative of a stable colloidal dispersion. The results of potentiometric titration (Fig. 3) indicated that the isoelectric point of n-TiO<sub>2</sub> was 4.1.

XR diffraction analysis showed that the material consisted chiefly of anatase and rutile. A recent study found that composition ranged from 73-85 % anatase, 14-17 % rutile and 0-18 % amorphous TiO<sub>2</sub> [40].

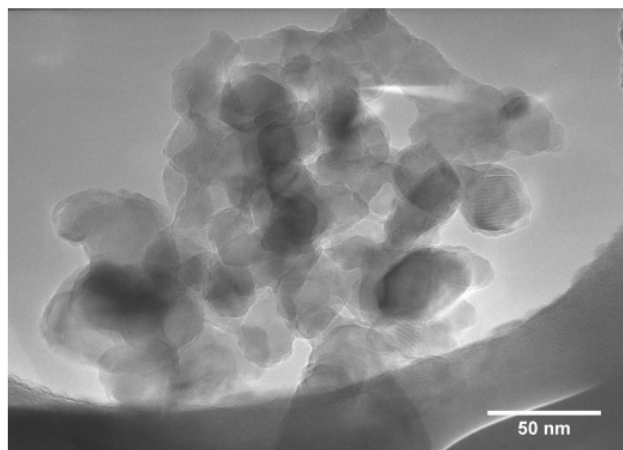


**Figure 1.** Transmission electron microscopy image of the n-TiO<sub>2</sub>.

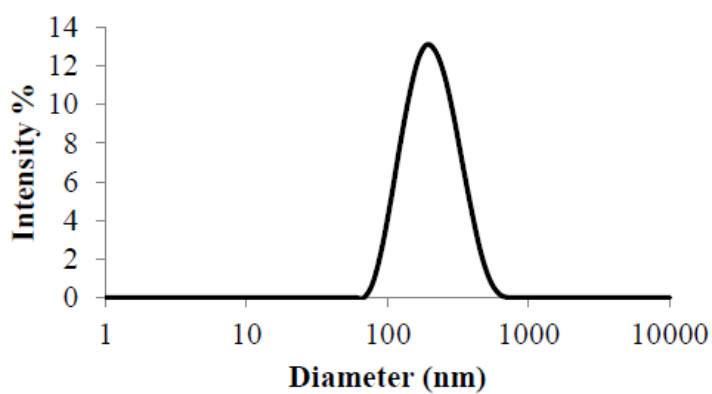


**Figure 2.** Particle size distribution of the nano-TiO<sub>2</sub>.

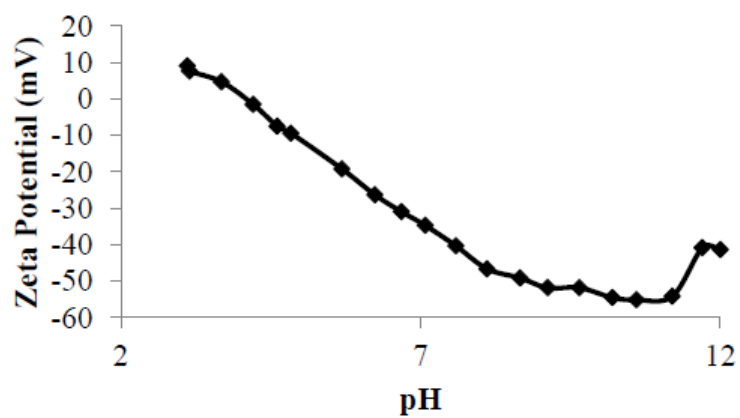


**Figure 3.** Zeta potential of n-TiO<sub>2</sub> as a function of pH.

### C.ii) Sand characterization

The physical structure and surface properties of granular media is a major factor determining the retention of colloidal material during porous media filtration. A more porous material may allow for additional surface area or more dead volume for the NPs to become trapped in. Also, a rougher material provides a more tortuous path for the NPs which increases physical entrapment. Scanning electron microscopy analysis confirmed that the sand used had a smooth surface and was non-porous. In agreement with these observations, the surface area of the sand (BET technique) was very low ( $< 0.05 \text{ m}^2/\text{g}$ ). Surface charge measurements at different pH values revealed that the apparent surface charge of sand is negative across circum-neutral and high pH ranges. The surface charge at pH 7 is of particular interest as that is the operating pH of the column experiments. At that pH value, sand has a highly negative surface charge ( $-21.68 \text{ C m}^{-2}$ ). The isoelectric point determined for the sand was 3.45.

### C.ii) Fate and transport of $\text{TiO}_2$ NPs in porous media: Impact of reclaimed water

Three contaminants were used to simulate varying contaminants commonly found in aqueous streams. An ammonium polyacrylate surfactant (Dispex A40) was selected as a model surfactant and dispersant. Lysozyme and glycine are two model organic compounds with disparate points of zero charge ( $\text{pH}_{\text{pzc}}$ ), 9.60 and 5.97, respectively [41-42]. The choice of organic compounds with respective  $\text{pH}_{\text{pzc}}$  values above and below the tested pH of 7.0 provided information that can be used to predict the interaction of positively and negatively charged organic molecules with n- $\text{TiO}_2$ .

Table 1 lists the average particle size and zeta potential of n- $\text{TiO}_2$  before and after addition of the three model contaminants. When no contaminant was added, the n- $\text{TiO}_2$  showed a consistent average particle size of 200 nm. While NP dispersions amended with Dispex and glycine displayed little departure from the virgin material, lysozyme showed significant potential for inducing n- $\text{TiO}_2$  aggregation (Fig. 4). The NP dispersion amended with lysozyme rapidly aggregated to approximately 350 nm and then slowly trended toward 500 nm. The rapid aggregation observed in assays with lysozyme is consistent with the zeta potential shift induced by the protein.

**Table 1.** Zeta potential of  $\text{TiO}_2$  nanoparticles in the presence and absence of organic additives at pH 7.0.

Solution	Zeta Potential (mV)
No Contaminant	$-41.7 \pm 3.7$
Dispex	$-50.5 \pm 2.5$
Lysozyme	$17.6 \pm 2.3$
Glycine	$-43.2 \pm 2.8$

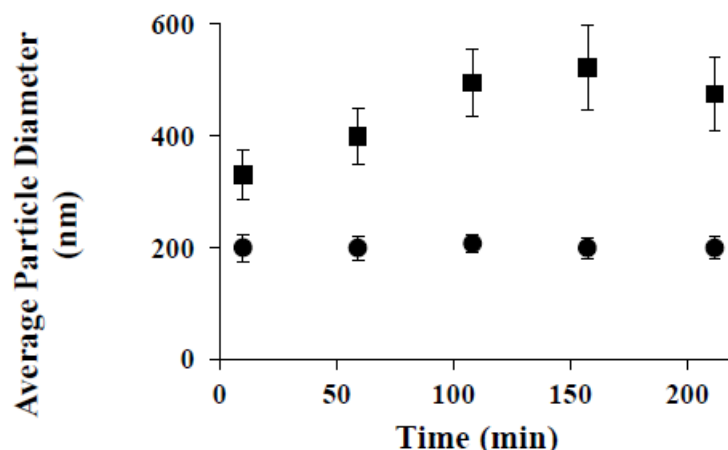


**Figure 4.** Average hydrodynamic diameter of n-TiO<sub>2</sub> aggregates as a function of time for the cases of no contaminant (●) and lysozyme (■).

While the zeta potential was -41.7 mV in assays lacking contaminant, there was a positive shift when lysozyme was added (17.6 mV). This shift is due to the net positive charge of the NP surface which results from sorption of lysozyme which is positively charged at pH 7 (high  $pH_{pzc}$  of 9.60). It is generally held that NP suspensions with a zeta potential less than 20 mV in magnitude will readily aggregate. The polyacrylate dispersant caused only a small reduction in the average size of TiO<sub>2</sub>, 195 nm, which corresponds to the further reduction in zeta potential, -50 mV. Glycine addition only caused a slight decrease in zeta potential (-43.2 mV). This decrease corresponds with the expected negative charge of glycine ( $pH_{pzc}$  = 5.97) at pH 7.

### *C.iii) Adsorption Isotherms*

There are four major mechanisms for NP capture in porous media: sedimentation, interception, straining, and diffusion or selective adsorption [44]. The first three are physical interactions determined to a large extent by the structure and packing of the porous material, while diffusion or selective adsorption is controlled by surface interactions. In order to separate physical interactions from surface adsorption, batch isotherms were performed with n-TiO<sub>2</sub> and sand (Fig. 5). Sand displayed very low affinity for n-TiO<sub>2</sub> at pH 7. For example, at an equilibrium concentration of approximately 50 mg TiO<sub>2</sub>/L, the n-TiO<sub>2</sub> loading determined for sand was only 0.02 mg TiO<sub>2</sub>/g medium. The low adsorption capacity observed was expected given the negative surface charge of sand and n-TiO<sub>2</sub> under circum-neutral pH conditions.

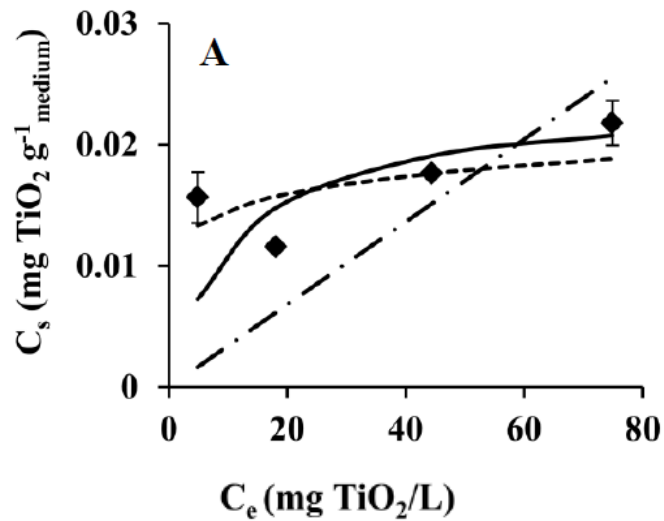


**Figure 5.** Association isotherms for n-TiO<sub>2</sub> onto sand. Henry (— · —), Freundlich (---), and Langmuir (—) isotherm fits.

**C.iv) Fate and Transport of TiO<sub>2</sub> NPs during Porous Media Filtration**

Figure 6 compares the relative effluent NP concentration with respect to time determined for n-TiO<sub>2</sub> dispersions in flow-through column experiments packed with sand. Plots of the NP concentrations associated with the filtration medium as a function of relative bed depth are shown in Figure 7. Sand was highly ineffective as an adsorbent material, with breakthrough being reached in less than two bed volumes (Fig. 6). Sand had a very small surface area and very little surface roughness, so physical interactions are unlikely to play a major role in retention under these conditions. This curve does match well with DLVO predictions, with the repulsive electrostatic interaction between the negatively charged n-TiO<sub>2</sub> and the negatively charged sand surface greatly outweighing the attractive van der Waals interactions.

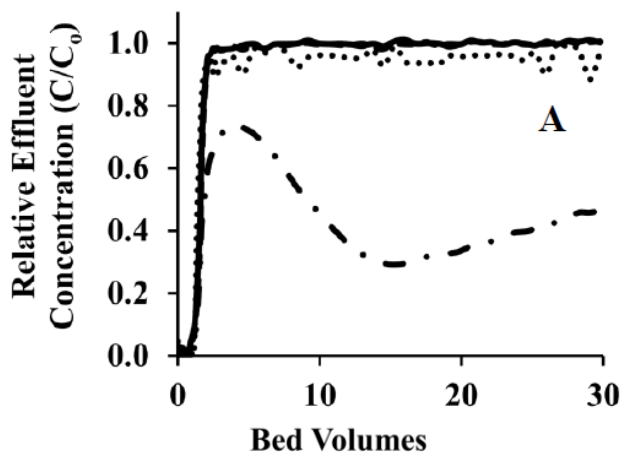


**Figure 6.** Relative effluent n-TiO<sub>2</sub> concentration as a function of the number of bed volumes processed for sand. Plots for dispersions with no contaminant (—), and for dispersions amended with Dispex (---), lysozyme (— · —), and glycine (···).



The captured NP concentration is extremely low; around 0.01 mg TiO<sub>2</sub>/g sand for the entire bed length (Fig. 7). Overall, the physical characteristics of sand do not aid in the retention of the n-TiO<sub>2</sub> and the repulsive electrostatic interactions dominate resulting in essentially zero retention [45-47].

**C.v) Effect of solution contaminants on n-TiO<sub>2</sub> fate and transport during porous media filtration**

The presence of organic contaminants impacted the transport and retention of n-TiO<sub>2</sub> in saturated sand columns. The model dispersant, Dispex, proved to be very effective in reducing n-TiO<sub>2</sub> retention during bed filtration. Although no departure from the baseline lacking Dispex can be observed for the sand bed (Fig. 6) due to the overall poor retention of sand, the impact of Dispex on NP retention was clearly observed in the columns packed with activated carbon (results not shown), with immediate full breakthrough for n-TiO<sub>2</sub> dispersions amended with the dispersant. Other dispersants have been shown to decrease NP retention [48-49] and studies have concluded this to be due to steric hindrances due to the adsorbed species [47,50]. Figure 7 shows the profiles of n-TiO<sub>2</sub> retained in the sand bed. This data supports the effluent concentration curves as the dispersant-contaminated n-TiO<sub>2</sub> is consistently the least retained in all bed materials.

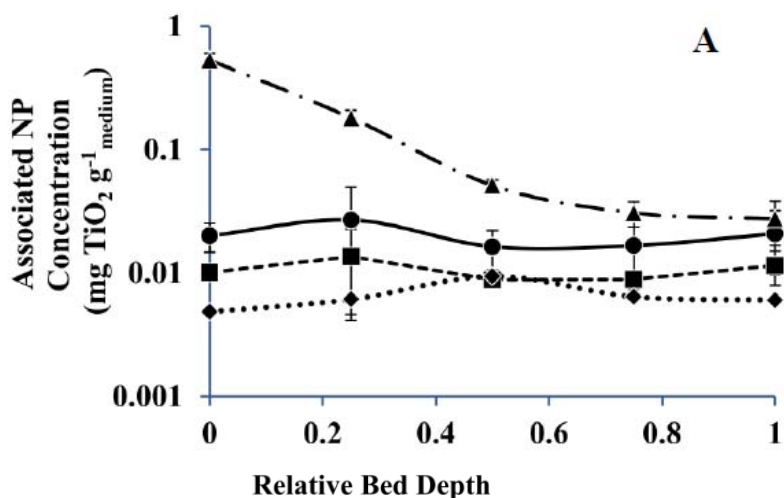


**Figure 7.** TiO<sub>2</sub> nanoparticle concentrations associated with porous media as a function of bed depth for sand. Four cases shown: no contaminant (---○---), Dispex (---■---), lysozyme (---▲---) and glycine (---◆---).

Addition of glycine did not lead to significant departure from the baseline case without contaminants in size or zeta potential, nor did it change the retention behavior in sand beds. In contrast, lysozyme greatly influenced n-TiO<sub>2</sub> retention. Results for lysozyme addition to the NP dispersion with sand as the filtration medium provide an excellent model case for filter ripening (Fig. 6). Here, as the lysozyme-coated NPs associate with the sand surface, the NPs themselves, destabilized by the addition of lysozyme onto their surface, become more efficient collectors than the bare sand surface, providing the characteristic “hump” in the breakthrough curve. While destabilization due to lysozyme addition did add to NP retention, a significant fraction of the n-TiO<sub>2</sub> eluted from the column. The retained n-TiO<sub>2</sub> bed profile for lysozyme contamination on the sand bed displayed a linear decrease over the bed length (Fig. 7), which exposes an

exponential decay characteristic of strong interactions between adsorbent and adsorbate. This could be either due to capture approaching capacity before moving down the column in the classical “front” or due to physical straining occurring near the inlet of the column. Due to the highly aggregated state of the lysozyme coated n-TiO<sub>2</sub> (> 500 nm); physical straining is the more likely cause.

The combined results of the contaminants and the variability in their effects displays the importance of a comprehensive investigation of any targeted wastewater stream to determine the competing roles the varying contaminants contained will play.

### ***C.vi) Environmental Implications***

A recent study has predicted that almost 3,000 tons of n-TiO<sub>2</sub> are released yearly from production, manufacturing and consumption in the United States alone [51]. This, combined with the increasing public concern about the safety of nanomaterials indicates the importance of understanding the environmental fate of n-TiO<sub>2</sub> and other nanomaterials. Improved knowledge of the behavior of engineered nanomaterials in porous media is particularly important since aquifer recharge with treated wastewater has the potential to introduce NPs into groundwater resources.

The results of n-TiO<sub>2</sub> transport experiments in saturated sand media confirmed that organic contaminants can have a strong impact on the transport and retention of nanoparticles. In the absence of organic contaminants, n-TiO<sub>2</sub> was poorly retained by the sand bed. The mobility of n-TiO<sub>2</sub> was altered to various degrees when model organic compounds were present in solution. This is due to the impact of organic additives on the stability of nanoparticle dispersions as well as the interaction between NP-granular media. In addition to organic contaminants, the presence of inorganic ionic species in treated wastewater is known to impact the state of aggregation and mobility of nanoparticles in saturated porous media [24]. In conclusion, these results indicate that the ultimate fate of nanomaterials during aquifer discharge will strongly depend on the composition of the treated wastewater. The nature of the nanomaterial considered and properties of the subsurface media should also be expected to impact nanoparticle-geomedia interactions and, thus, the ultimate fate of engineered nanomaterials during aquifer recharge with treated wastewater.

## **E. Literature**

- [1] R.J. Aitken, M.Q. Chaudhry, A.B.A. Boxall, M. Hull, Manufacture and use of nanomaterials: current status in the UK and global trends, *Occupational Medicine-Oxford*, 56 (2006) 300-306.
- [2] Anonymous, Nanotechnology Consumer Product Inventory. Washington, DC: Project on Emerging Nanotechnologies, Woodrow Wilson International Center for Scholars and the Pew Charitable Trusts. Available at <http://www.nanotechproject.org/consumerproducts>, (2011).
- [3] J. Sass, Nanotechnology’s invisible threat: Small science big consequences, In: NRDC Issue Paper, Natural Resources Defense Council, New York, NY, USA, 2007.
- [4] S.J. Klaine, P.J.J. Alvarez, G.E. Batley, et al., Nanomaterials in the environment: Behavior, fate, bioavailability, and effects, *Environ. Toxicol. Chem.*, 27 (2008) 1825-1851.

- [5] D.O. Volkov, P.R.V. Dandu, H. Goodman, et al., Influence of adhesion of silica and ceria abrasive nanoparticles on chemical-mechanical planarization of silica surfaces, *Appl. Surface Sci.*, 257 (2011) 8518-8524.
- [6] J. Wang, A.G. Haerle, Chemical mechanical planarization of copper using transition alumina nanoparticles, *Thin Solid Films*, 516 (2008) 7648-7652.
- [7] J.M. Balbus, A.D. Maynard, V.L. Colvin, et al., Meeting report: Hazard assessment for nanoparticles - Report from an interdisciplinary workshop, *Environ. Health Perspect.*, 115 (2007) 1654-1659.
- [8] M.R. Gwinn, V. Vallyathan, Nanoparticles: Health effects - Pros and cons, *Environ. Health Perspect.*, 114 (2006) 1818-1825.
- [9] R.D. Handy, F. von der Kammer, J.R. Lead, et al., The ecotoxicology and chemistry of manufactured nanoparticles, *Ecotoxicology*, 17 (2008) 287-314.
- [10] B. Nowack, T.D. Bucheli, Occurrence, behavior and effects of nanoparticles in the environment, *Environ. Pollut.*, 150 (2007) 5-22.
- [11] G. Oberdorster, V. Stone, K. Donaldson, Toxicology of nanoparticles: A historical perspective, *Nanotoxicology*, 1 (2007) 2-25.
- [12] G. Oberdörster, A. Maynard, K. Donaldson, et al., Principles for characterizing the potential human health effects from exposure to nanomaterials: elements of a screening strategy, *Particle Fibre Toxicol.*, 2 (2005) 8.
- [13] W.G. Kreyling, M. Semmler-Behnke, W. Moller, Health implications of nanoparticles, *J. Nanoparticle Res.*, 8 (2006) 543-562.
- [14] L.K. Limbach, Y.C. Li, R.N. Grass, et al. Oxide nanoparticle uptake in human lung fibroblasts: Effects of particle size, agglomeration, and diffusion at low concentrations, *Environ. Sci. Technol.* 39 (2005) 9370-9376.
- [15] J.X. Wang, G.Q. Zhou, C.Y. Chen, et al., Acute toxicity and biodistribution of different sized titanium dioxide particles in mice after oral administration, *Toxicol. Lett.*, 168 (2007) 176-185.
- [16] M. Auffan, J.Y. Bottero, C. Chaneac, J. Rose, Inorganic manufactured nanoparticles: how their physicochemical properties influence their biological effects in aqueous environments, *Nanomedicine*, 5 (2010) 999-1007.
- [17] A.B. Boxall, K. Tiede, Q. Chaudhry, Engineered nanomaterials in soils and water: How do they behave and could they pose a risk to human health?, *Nanomedicine*, 2 (2007) 919-927.
- [18] N.C. Mueller, B. Nowack, Exposure modeling of engineered nanoparticles in the environment, *Environ Sci Technol*, 42 (2008) 4447-4453.
- [19] M.A. Kiser, P. Westerhoff, T. Benn, et al., Titanium nanomaterial removal and release from wastewater treatment plants, *Environ. Sci. Technol.*, 43 (2009) 6757-6763.
- [20] B. Kim, C.S. Park, M. Murayama, et al., Discovery and characterization of silver sulfide nanoparticles in final sewage sludge products, *Environ. Sci. Technol.*, 44 (2010) 7509-7514.
- [21] T.M. Benn, P. Westerhoff, Nanoparticle silver released into water from commercially available sock fabrics, *Environ. Sci. Technol.*, 42 (2008) 4133-4139.
- [22] L.K. Limbach, R. Bereiter, E. Muller, et al., Removal of oxide nanoparticles in a model wastewater treatment plant: influence of agglomeration and surfactants on clearing efficiency, *Environ Sci Technol*, 42 (2008) 5828-5833.

- [23] F. Gomez-Rivera, J.A. Field, D. Brown, R. Sierra-Alvarez, Fate of cerium dioxide nanoparticles in municipal wastewater during activated sludge treatment, *Bioresource Technol.* (In press). (2011).
- [24] A.R. Petosa, D.P. Jaisi, I.R. Quevedo, et al., Aggregation and deposition of engineered nanomaterials in aquatic environments: Role of physicochemical interactions, *Environ. Sci. Technol.*, 44 (2010) 6532-6549.
- [25] K. Rezwani, A.R. Studart, J. Voros, L.J. Gauckler, Change of zeta potential of biocompatible colloidal oxide particles upon adsorption of bovine serum albumin and lysozyme, *J. Phys. Chem.*, B109 (2005) 14469-14474.
- [26] E. Tombacz, Z. Libor, E. Illes, et al., The role of reactive surface sites and complexation by humic acids in the interaction of clay mineral and iron oxide particles, *Org. Geochem.*, 35 (2004) 257-267.
- [27] J.J. Lu, X.M. Yan, Y.M. Zhou, et al., Comparative study of the adsorption capacity of peat humic acid (PHA) and soil humic acid on nano-SiO<sub>2</sub> and nano-kaolin, *Fresenius Environ. Bull.*, 18 (2009) 346-352.
- [28] J. Gao, S. Youn, A. Hovsepian, et al., Dispersion and toxicity of selected manufactured nanomaterials in natural river water samples: effects of water chemical composition, *Environ. Sci. Technol.*, 43 (2009) 3322-3328.
- [29] Metcalf & Eddy, *Wastewater Engineering: Treatment and Reuse*, Tchobanoglous, G., Burton, F. L., Stensel, H. D. (Eds.). 4th Edition. McGraw Hill, Boston, (2003).
- [30] R.A. French, A.R. Jacobson, B. Kim, et al., Influence of ionic strength, pH, and cation valence on aggregation kinetics of TiO<sub>2</sub> nanoparticles, *Environ. Sci. Technol.* 43 (2009) 1354-1359.
- [31] S. Jailani, G.V. Franks, T.W. Healy, Zeta potential of nanoparticle suspensions: Effect of electrolyte concentration, particle size, and volume fraction, *J. Am. Ceram. Soc.*, 91 (2008) 1141-1147.
- [32] E.M. Hotze, T. Phenrat, G.V. Lowry, Nanoparticle aggregation: Challenges to understanding transport and reactivity in the environment, *J. Environ. Qual.*, 39 (2010) 1909-1924.
- [33] M. Rodriguez, J.A. Field, R. Sierra-Alvarez, Stability and aggregation of cerium dioxide nanoparticles in natural aqueous matrices. (Submitted for publication), (2013).
- [34] M.A.H. Cortazar, P. Behra, Sorption of silver(I) onto the surface of pure and natural quartz sands, *J. De Physique*, 107 (2003) 609-612.
- [35] APHA, *Standard methods for the examination of water and wastewater*. Clesceri, L. S et al. (eds.). 20th Ed. Washington D.C., American Public Health Association, 1998.
- [36] A.B.A. Boxall, Q. Chaudhry, C. Sinclair, et al., Current and future predicted environmental exposure to engineered nanoparticles. Central Science Laboratory, Department of the Environment and Rural Affairs, London, UK., (2007).
- [37] W. Zhang, Nanoscale iron particles for environmental remediation: An overview, *J. Nanopart. Res.*, 5 (2003) 323-332.
- [38] I. Chowdhury, Y. Hong, R.J. Honda, et al., Mechanisms of TiO<sub>2</sub> nanoparticle transport in porous media: Role of solution chemistry, nanoparticle concentration, and flowrate, *J. Coll. Interf. Sci.*, 360 (2011) 548-555.
- [39] S.R. Kanel, S.R. Al-Abed, Influence of pH on the transport of nanoscale zinc oxide in saturated porous media, *J. Nanoparticle Res.*, 13 (2011) 4035-4047.

- [40] Peters, K., R.E. Unger, C.J. Kirkpatrick, et al. Effects of nano-scaled particles on endothelial cell function in vitro: Studies on viability, proliferation and inflammation. *J. Mater. Sci-Mater in Medicine*, 2004. 15(4): 321-325.
- [41] Cheng, M.D. Effects of nanophase materials ( $\leq 20$  nm) on biological responses. *J. Environ Sci Health A-Toxic/Hazard Subst Environ Eng*, 2004. 39(10): 2691-2705.
- [42] Rahman, Q., M. Lohani, E. Dopp, et al. Evidence that ultrafine titanium dioxide induces micronuclei and apoptosis in syrian hamster embryo fibroblasts. *Environ Health Persp*, 2002. 110(8): 797-800.
- [43] Thill, A., O. Zeyons, O. Spalla, et al. Cytotoxicity of CeO<sub>2</sub> nanoparticles for *Escherichia coli*. Physico-chemical insight of the cytotoxicity mechanism. *Environ Sci Technol* 2006. 40(19): 6151-6156.
- [44] Hund-Rinke, K., M. Simon. Ecotoxic effect of photocatalytic active nanoparticles TiO<sub>2</sub> on algae and daphnids. *Environ Sci Pollut Res*, 2006. 13(4): 225-232.
- [45] Nowack, B., T.D. Bucheli. Occurrence, behavior and effects of nanoparticles in the environment. *Environ Pollut*, 2007. 150(1): 5-22.
- [46] Roco, M.C. Environmentally responsible development of nanotechnology. *Environ Sci Technol*, 2005. 39(5): 106A-112A.
- [47] Savage, N., M.S. Diallo. Nanomaterials and water purification: Opportunities and challenges. *J Nanoparticle Res*, 2005. 7(4-5): 331-342.
- [48] Bolis, V., C. Busco, M. Ciarletta, et al. Hydrophilic/hydrophobic features of TiO<sub>2</sub> nanoparticles as a function of crystal phase, surface area and coating, in relation to their potential toxicity in peripheral nervous system. *J Colloid Interf Sci*, 2012. 369: 28-39.
- [49] Lovern, S.B., R. Klaper. *Daphnia magna* mortality when exposed to titanium dioxide and fullerene (C-60) nanoparticles. *Environ Toxicol Chem*, 2006. 25(4): 1132-1137.
- [50] Federici, G., B.J. Shaw, R.D. Handy. Toxicity of titanium dioxide nanoparticles to rainbow trout (*Oncorhynchus mykiss*): Gill injury, oxidative stress, and other physiological effects. *Aquatic Toxicol*, 2007. 84(4): 415-430.
- [51] Ju-Nam, Y., J.R. Lead. Manufactured nanoparticles: An overview of their chemistry, interactions and potential environmental implications. *Sci Total Environ*, 2008. 400(1-3): 396-414
- [52] Rottman, J., R. Sierra-Alvarez, F. Shadman. Real-time monitoring of nanoparticle retention in porous media. *Environ Chem Lett*, (in press).